The American Journal of Pathology, Vol. 171, No. 2, August 2007

DOI: 10.2353/ajpath.2007.061138

Tumorigenesis and Neoplastic Progression

Hypoxia-Inducible Factor-1 Facilitates Cervical Cancer Progression in Human Papillomavirus Type 16 Transgenic Mice

Zhi Hong Lu,* Jason D. Wright,† Brian Belt,† Robert D. Cardiff,‡ and Jeffrey M. Arbeit*†§¶‖

From the Division of Urologic Surgery, the Department of Obstetrics and Gynecology,† Division of Gynecologic Oncology, the Department of Surgery,§ the Siteman Cancer Center,¶ and the Program in Cell Biology,‖ Washington University School of Medicine, St. Louis, Missouri; and the Center for Comparative Medicine,‡ University of California, Davis, California*

Advanced cervical cancer remains a vexing clinical challenge despite screening programs. Many of these cancers are hypoxic, and expression of the α subunit of the major regulator of the hypoxic cellular response, the transcription factor hypoxia-inducible factor-1 (HIF-1), is correlated with poor prognosis. Here, we tested a functional role for HIF-1α in pathogenesis of cervical cancer in estrogen-treated transgenic mice. Double-transgenic (DTG) mice developed locally invasive cervical cancers 70 times larger than K14-HPV16 mice. *In vivo* bromodeoxyuridine incorporation was elevated in DTG cancers without a significant increase in apoptosis. HIF-1α gain of function did not up-regulate canonical HIF-1 targets in premalignant DTG cervices, in contrast to elevation of these targets in K14-HIF-1α transgenic cervices. The DTG transcriptional signature included up-regulation of mRNAs encoding cytokines and chemokines, immune signaling molecules, extracellular proteases, and cell motility factors, as well as reduced expression of cell adhesion and epithelial differentiation genes. Importantly, a set of gene markers derived from the DTG transcriptome predicted cervical cancer progression in patients. This study suggests a novel paradigm for HIF-1 function evident in multistage carcinogenesis as opposed to established malignancies, including interaction with viral oncogenes to induce multiple genomic networks in premalignancy that fosters the development of advanced cervical cancer. *(Am J Pathol 2007, 171:667–681; DOI: 10.2353/ajpath.2007.061138)*

Cervical cancer is the second most common malignancy in women worldwide. More than 99% of cervical carcinomas are associated with human papillomavirus (HPV).[1] Viral persistence and hence carcinogenic disease progression are attributable to low-level HPV viral genome expression in basal keratinocytes of the uterine transformation zone.[2] Despite the promise of the HPV16/18 vaccine, the large cohort of currently infected women will be a continual source for cervical malignancies throughout the next 4 decades.[2] Screening programs have been successful in economically sufficient populations to reduce markedly cancer incidence; however, women with inadequate health care access continue to present with advanced local disease beyond the confines of the cervix.

A prominent feature of clinically advanced cervical cancers is hypoxia,[3,4] which is a therapeutic and prognostic factor associated with radioresistance, inhibition of apoptosis, alterations in proliferation, cell signaling, and genomic stability.[5–7] A central coordinator of the hypoxic cellular response is hypoxia-inducible factor-1 (HIF-1), a master transcription factor regulating expression of a growing list of downstream targets.[8,9] HIF-1 is a heterodimeric transcription factor composed of an oxygen-labile HIF-1α subunit and a constitutively expressed HIF-1β (ARNT) subunit. HIF-1 contains multiple domains, including an oxygen-dependent degradation (ODD) domain, responsible for protein stability and transcriptional activity. During normoxia, HIF-1α rapidly undergoes ubiquitin-mediated degradation, principally regulated by proline hydroxylation and further facilitated by acetyla-

Supported by the National Cancer Institute (grants R01-90722 to J.M.A. and T32CA 009621-17 to J.D.W.).

Z.H.L. and J.D.W. contributed equally to this study.

Accepted for publication April 24, 2007.

Supplemental material for this article can be found on *http://ajp.amjpathol.org*.

Current address of J.D.W.: Division of Gynecologic Oncology, Department of Obstetrics and Gyneology, Columbia University College of Physicians and Surgeons, New York, New York.

Address reprint requests to Zhi Hong Lu, Ph.D., 660 South Euclid, Box 8242, St. Louis, MO 63110. E-mail: luz@wudosis.wustl.edu.

tion, and negatively regulated by sumoylation of multiple amino acids within the ODD.[8,10,11] Prolines (Pro)^{402} and Pro^{564} within the ODD are principally responsible for protein stability.[10] Normoxic HIF-1α hydroxylation is catalyzed by specific prolyl hydroxylases. Pro^{402}/Pro^{564} hydroxylation presents binding sites for the von Hippel-Lindau (VHL) protein, the recognition component of an E3-ubiquitin ligase.[12] During hypoxia, HIF-1α prolyl and asparaginyl hydroxylases are inhibited, VHL-HIF binding is impaired, the majority of HIF-1α protein is stabilized, and consequent HIF-1 dimerization produces the transcriptionally active HIF-1.[8] HIF-1 binding to hypoxia response elements at enhancers of target genes increases the expression of molecules regulating angiogenesis, glucose transport, glycolysis, tissue invasion/metastasis, and cell proliferation.[8] Cancer cells also possess parallel mechanisms for normoxic HIF-1α protein stabilization and transcriptional activity including elevated HIF-1α protein translation because of increased phosphoinositol 3′ kinase pathway signaling,[13] RAS/MEK/ERK-1/2-mediated phosphorylation of HIF-1α[14] and coactivator CBP/p300,[15] as well as microenvironmental acidosis, which sequesters VHL in the nucleolus.[16]

Multiple clinical studies of cervical carcinogenesis have suggested that HIF-1α is important in malignant progression and outcome.[3,17,18] Likewise, HIF-1α has been proposed as a facilitator of clinical premalignant progression because immunohistochemical expression of HIF-1α and its targets were incrementally increased in patients with advancing degrees of cervical dysplasia.[17] Modulation of HIF-1α expression has been restricted to allograft studies of either ARNT-deficient mouse Hepa c4 hepatoma cells[19] or SV40 Tag/Ha-ras-transformed MEFs from HIF-1α knockout mice.[20] The Hepa c4 allograft model highlighted a decrease of tumor microvasculature associated with diminished expression of the HIF-1 target vascular endothelial growth factor (VEGF), whereas the HIF-1α knockout MEF study suggested that HIF-1 mediated tumor growth through VEGF-independent changes in either cellular metabolism or the microenvironment. Despite the elegance of these genetic studies, human disease is characterized by HIF-1 gain of function, and this pivotal experiment has not been genetically tested in a mouse model of multistage carcinogenesis.

Here, we tested the hypothesis that HIF-1α gain of function would alter cervical carcinogenesis in a mouse model closely emulating human cervical carcinogenesis, the estrogen-treated K14-HPV16 transgenic mouse.[21,22] Double-transgenic (DTG) mice expressing both HPV oncogenes and constitutively active HIF-1α mutants in cervical epithelium developed massive cervical cancers that replaced the entire cervix and invaded peri-cervical soft tissue, emulating locally advanced disease in humans. In contrast, cancers in single K14-HPV16 transgenic mice were always microscopic. DTG cervical cancers had an elevated rate of proliferation without a differential compensatory increase in apoptosis. Strikingly, DTG cancers did not display an increase in vascularity in contrast to our previous work in an epidermal transgenic model of HIF-1α gain of function.[23] Genome-wide gene expression screening of premalignant cervical dysplasia midway in the progression of disease in the model revealed a segregation of nontransgenic, HPV single transgenic, and DTG cervices into three distinct clusters. A subset of the DTG signature transcriptome derived from the mouse model was also able to discriminate advanced human cervical cancers as well. Thus, a distinct molecular expression network is activated by the combination of HPV16 oncogene expression with HIF-1α gain of function setting the stage, in premalignancy, for the ultimate elaboration of advanced cervical cancer.

Table 1. Number of Mice of Each Genotype

Genotype	Number	Cancer incidence (%)
Nontransgenic	8	0
K14-HIF-1$\alpha\Delta$ODD and HIF-1αPro$^{402A/564G}$	7	0
K14-HPV16	15	12 (80)
K14-HPV16:HIF-1$\alpha\Delta$ODD	6	6 (100)
K14-HPV16:HIF-1αPro$^{402A/564G}$	8	6 (75)

Because no neoplastic pathology developed in nontransgenic or K14-HIF-1α constitutive mutants, the analysis focused on comparisons between the K14-HPV16 and K14-HPV16:HIF-1$\alpha\Delta$ODD and K14-HPV16:HIF-1αPro$^{402A/564G}$ double-transgenic mice.

Materials and Methods

Transgenic Mice

K14-HPV16 transgenic mice (n = ~100 in FVB/n)[22] were mated with transgenic mice with two different constitutively active HIF-1 transgenes, either K14-HIF-1$\alpha\Delta$ODD transgenic mice (FVB/n original background strain)[23] or a new line of mice transgenic animals (also FVB/n) with HIF-1α containing proline to alanine and proline to glycine mutations at positions 402 and 564, respectively (K14-HIF-1Pro$^{402A/564G}$) (M. Scortegagna and J.M.A., in preparation), producing K14-HPV16:HIF-1$\alpha\Delta$ODD and K14-HPV16:HIF-1αPro$^{402A/564G}$ DTG mice.[21–24] Negative littermate FVB/n, K14-HPV16, and K14-HIF-1αPro$^{402A/564G}$ transgenic mice served as controls (Table 1). The Animal Studies Committee of the Washington University in St. Louis, MO, approved all animal manipulations.

Histology

Mice were anesthetized with 2.5% tribromoethanol (Aldrich, St. Louis, MO), the left ventricle-cannulated with a 22-gauge gavage needle (no. 01-290-2A; Fisher Scientific, St. Louis, MO), perfused first with 10% sucrose at 150 mmHg for 1 to 2 minutes, to clear blood and osmotically equilibrate the tissue, followed by 10% formalin for 3 minutes, (Perfusion One Rodent System; McCormick Scientific, St. Louis, MO). The entire reproductive tract (vagina, cervix, and uterine horns) as well as lymph nodes, chest skin, and ear control tissue were harvested from 6-month estrogen-treated mice.[22] Tissues underwent rapid microwave fixation in 10% formalin for 1 hour (Pelco Biowave DFR-10 tissue processor; Ted Pella Co., Redding, CA), allowing precise wattage and temperature

control (45 minutes, 169 W, 22°C; and 15 minutes, 647 W, 32°C) and rapid *in situ* formaldehyde generation. After a phosphate-buffered saline (PBS) wash, processing through graded alcohols and xylenes, and paraffin embedding, 5-μm tissue sections were obtained for histopathology using staining with hematoxylin and eosin or immunohistochemistry.[22] Cancer size was determined by measuring the greatest two perpendicular diameters and multiplying them together to obtain an area value in mm^2. The results were expressed as mean ± SEM and analyzed using both the Student's *t*-test and the nonparametric Mann-Whitney *U*-test.

Immunohistochemistry

In vivo tissue proliferation kinetics was performed using 5-bromo-2′-deoxyuridine (BrdU) injection and immunohistochemical analysis as described previously.[22] Tissue sections were stained with a polyclonal antibody for activated cleaved caspase-3 (no. 9661; Cell Signaling Technology, Beverly, MA) and for CD31 (no. 550274; BD Pharmingen, San Diego, CA) using antigen retrieval in 1× Reveal solution, pH 6.0 (Biocare Medical, Concord, CA), and pressure cooked for 4 minutes at 125°C and 10 seconds at 90°C (Biocare medical decloaking chamber). After a water and serial PBS wash, endogenous peroxidase was blocked with 3% hydrogen peroxide in methanol for 10 minutes, protein blocked, and the primary antibody incubated overnight at 4°C. PBST-washed slides were incubated with goat anti-rabbit antibody, 1:200, (antibody diluent; DAKO, Carpinteria, CA), followed by ABC reagent (Vector Elite, PK-6100; Vector Laboratories, Burlingame, CA), 3,3′-diaminobenzidine (no. K3468; DAKO) and counterstaining with Meyer's hematoxylin. Both BrdU and cleaved caspase-3 immunohistochemistry were quantified using an Olympus BX-61 microscope, an Olympus DP70 charge-coupled device camera (Olympus, Melville, NY), and MicroSuite Biological Suite software (Soft Imaging System, Lakewood, CO). Regions were counted based on tissue histopathology and initial visual estimation of positive nuclei multiplicity for either BrdU or activated caspase-3. Images, ×400 magnification, were captured and labeled, and total number of cells was manually determined using the touch-count software function. Where the size of the cancer allowed, six fields were photographed and counted. However, fewer fields were available in some microscopic single K14-HPV cancers. Both unpaired Student's *t*-test and nonparametric Mann-Whitney *U*-tests were used to determine statistical significance (Prism 4; GraphPad Software, San Diego, CA).

Microarray Analysis

Uterine horns and lower vagina were removed from the cervix and upper vagina of nontransgenic ($n = 6$), single-transgenic ($n = 6$), and double-transgenic ($n = 5$) mice treated with estrogen for 3 months. The cervix and upper vagina were snap-frozen in liquid nitrogen and homogenized in TRIzol reagent (Invitrogen, Carlsbad, CA); total RNA was isolated using the manufacturer's guidelines and treated with RQ1 DNase (Promega, Madison, WI) for 30 minutes at 37°C. Microarray probes were synthesized using RNA samples from individual mice and hybridized with Affymetrix MU430Av2 GeneChips in the Siteman Cancer Center Multiplexed Gene Analysis Core. The dataset was first analyzed identifying probe sets scored as absent (ie, not detected) for all samples, which were excluded from analyses. Expressed probe sets were hierarchically clustered using the Spotfire DecisionSite software. Normalized *z*-scores of individual datasets were analyzed with unsupervised Euclidean distance-based clustering and with three-way principal component analysis. Significance analysis of microarrays (SAM analysis) was next used to identify differentially expressed transcripts. Two-class unpaired permutation testing using a twofold-change threshold determined significant expression differences. Analysis stringency (ie, the predicted median false discovery rate) was adjusted using a statistical tuning parameter (Δ value) and was indicated in each experiment. Unpaired *t*-tests were also performed to identify additional differentially expressed transcripts. Biological pathway analysis was delineated using a gene ontology-based program (Spotfire DecisionSite).

Quantitative Real-Time Reverse Transcriptase-Polymerase Chain Reaction (RT-PCR)

Quantitative real-time RT-PCR was performed as described previously using a MX3000P thermocycler and detection system (Stratagene, La Jolla, CA). Primer Express software (version 2.0; Applied Biosystems, Foster City, CA) was used to design primer/probe sets (Supplemental Table S1, see *http://ajp.amjpathol.org*), and target cDNAs were normalized to histone 3.3A.[23] Statistical significance was determined as described above.

Results

Cervical Cancer Incidence

Production of adult DTG mice was technically challenging because of increased perinatal mortality as a result of an additive skin phenotype from both transgenic models consisting of HPV16-induced epidermal hyperplasia, angiogenesis, and inflammation combined with the angiogenesis and inflammation induced by HIF-1α gain of function. Fourteen surviving DTG mice along with 15 K14-HPV16 (HPV16) littermate controls were treated with our protocol for estrogen-induced cervical carcinogenesis.[22] Reproductive tract histopathological analysis identified invasive squamous cell carcinomas in 12 of 14 DTG mice (85.7%) and high-grade cervical dysplasia in the remainder (14.3%) (Table 1). Cervical malignancies were documented in 12 of 15 HPV16 controls (80%), with three evidencing cervical intraepithelial neoplasia III (CINIII, 20%). Thus, gain of HIF-1α function did not alter cervical cancer incidence or multiplicity when compared with concurrent HPV16 controls.[21,22] There were no signifi-

cant differences in tumor incidence, histopathology, or the penetrance of advanced invasive carcinomas between the DTG mice carrying either of the two HIF-1α mutant genes (Table 1, and data not shown). As neither nontransgenic controls nor K14-HIF-1α mutant transgenic mice displayed pathology other than estrogen-induced squamous hyperplasia (Table 1 and Supplemental Figure 1, see *http://ajp.amjpathol.org*), they were not subject to further histopathological analysis. None of the mice from any of the transgenic genotypes developed cervical cancer without estrogen, consistent with our previous experience.[22] Finally, the skin cancer incidence was not different between single HPV16 compared with DTG mice (data not shown).

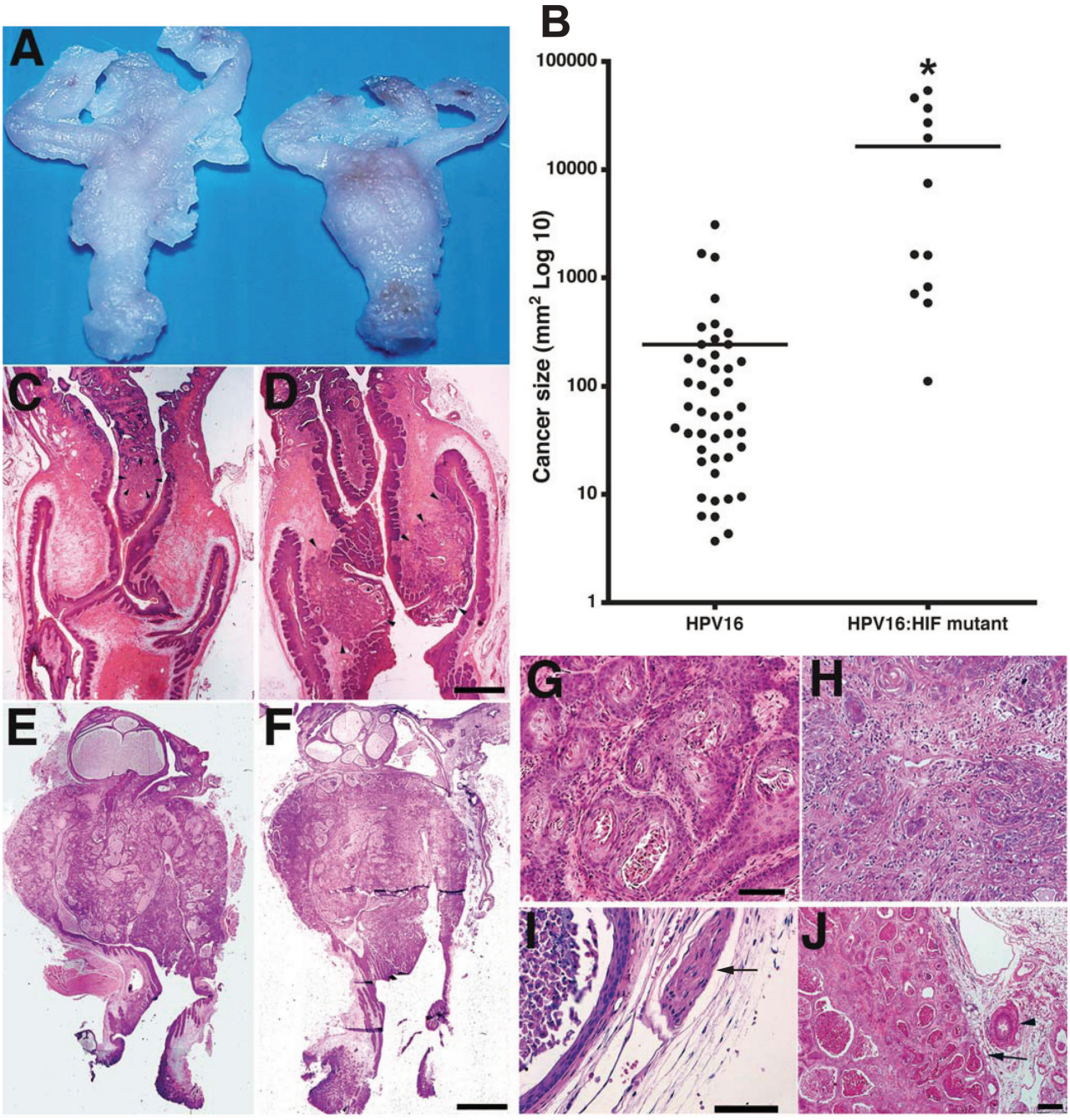

Figure 1. Cervical cancer histopathology. **A:** Gross morphology of reproductive tracts from a K14-HPV16 mouse (left) and a K14-HPV-HIF-1 DTG mouse (right). **B:** Log10 scatter plot of tumor area of cancers from HPV16 and DTG mice demonstrates the size variability of the HPV16 cervical cancers and the striking bimodal population of DTG cancers; bars represent mean tumor planar area. **C** and **D:** Overviews of the cervix and upper vagina from two HPV16 mice. Both have small, invasive squamous carcinomas; one (**C**, **arrowhead cluster**) localized to the cervical transformation zone, typical of the original model, and the other displaying more extensive stromal invasion on both sides of the cervix (**D**, **arrowheads**), also seen previously in the model. **E** and **F:** Overviews of the reproductive tracts of two DTG mice demonstrate the huge size and local invasion of the cervical cancers. **G** and **H:** DTG cancers are markedly heterogeneous with well-differentiated (**G**) and poorly differentiated (**H**) regions within the same large cancer. **I** and **J:** DTG malignant parametrial invasion encroaches on nerves (**I**, **arrow**) and the ureter (**J**, **arrowhead**). Scale bars: 0.9 mm (**C** and **D**); 2 mm (**E** and **F**); 150 μm (**G** and **H**); 25 μm (**I**); 200 μm (**J**). Original magnifications, ×1.25 (**C** and **D**).

Cervical Cancer Histopathology

Twelve cervical squamous cancers from DTG mice were compared with 45 cancers from concurrent and archival HPV16 mice.[22] A subset of DTG cancers displayed visible cervical enlargement, a characteristic never before observed in this mouse model (Figure 1A). Quantitative analysis of cervical cancer area demonstrated a 70-fold size increase in DTG malignancies (16.4 ± 5.7 mm^2) compared with K14-HPV16 counterparts (0.24 ± 0.10 mm^2), with a bimodal size distribution of the DTG cancers (Figure 1B, $P = 0.0001$). We focused further histopathological analysis on the massive (>5.0 mm^2) DTG cancers versus the larger HPV16 cervical malignancies. All HPV16 single-transgenic squamous cancers were microscopic, well differentiated, and variable in size (Figure 1, C and D), consistent with our previous experience.[22] In contrast, DTG cervical cancers were locally expansile, obliterated the entire cervix, and invaded the upper half of the vagina (Figure 1, E and F). DTG cancers were also heterogeneous, particularly at the invasive periphery, containing both well-differentiated regions containing invasive squamous cancer cells arrayed in keratin pearls (Figure 1G), and poorly differentiated areas consisting of clustered malignant squamous cells invading a desmoplastic stroma (Figure 1H). DTG cancers often penetrated the cervical serosa into the adjacent parametrial tissue and encroached on the pelvic nerves and ureter (Figure 1, I and J, arrows and arrowheads, respectively). Importantly, DTG mice did not evidence regional metastases to the pelvic or para-aortic lymph nodes, or systemic spread to other organs even in mice with massive cervical malignancies. Collectively, these data suggested that HIF-1α gain of function promoted local growth and parametrial invasion of cervical cancer phenocopying clinically advanced disease and also that additional independent molecular events coordinate metastasis.

It is worth noting that there was no histological evidence for an increase in vascularity in either massive or smaller DTG cervical cancers compared with HPV16 counterparts (Figure 1, G–J; and data not shown). Immu-

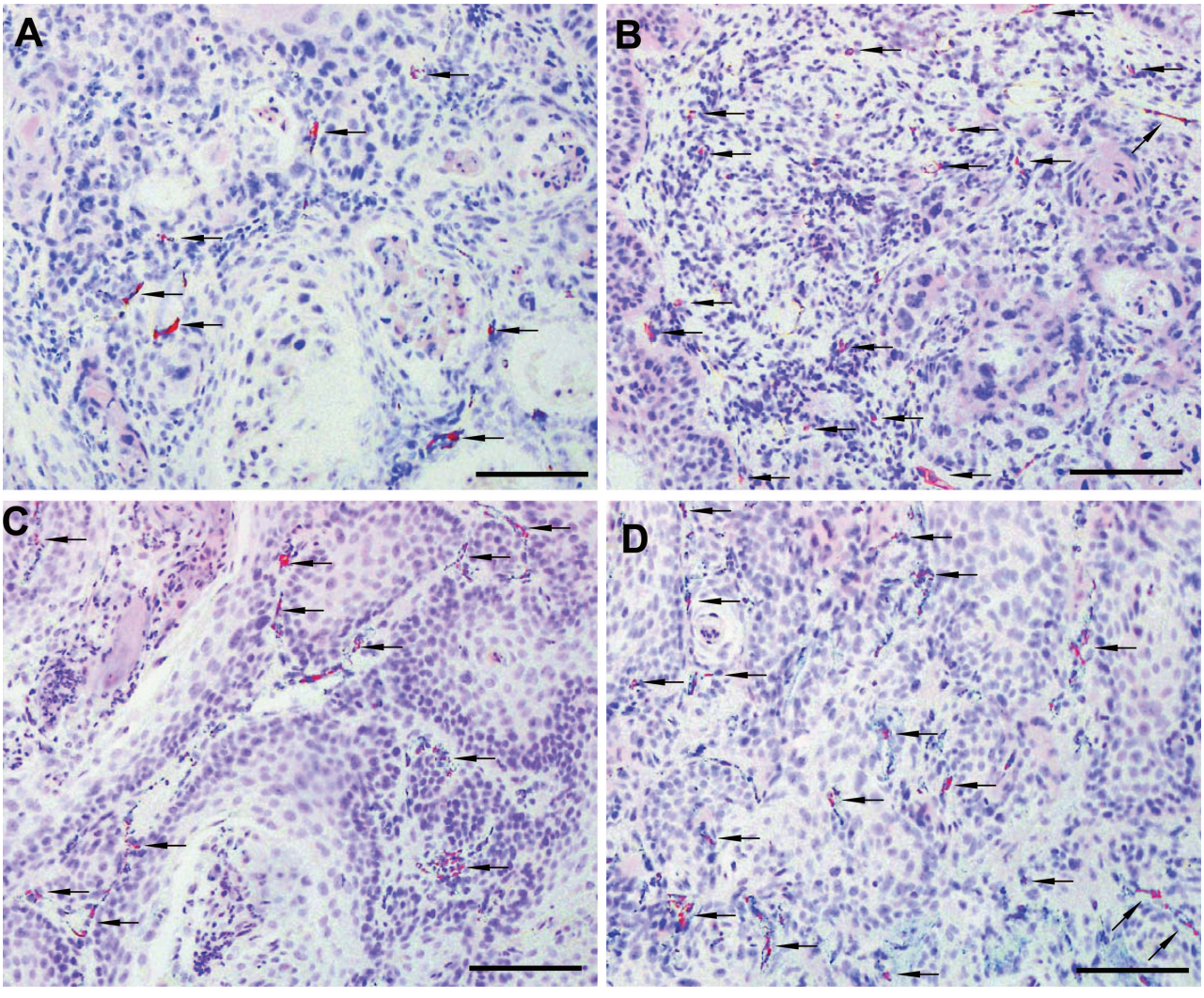

Figure 2. Immunohistochemical analysis of expression of the vascular marker CD31 in cervical carcinomas. **A** and **B:** Two separate high-power views of one HPV16 cervical cancer. **C** and **D:** Two separate high-power views of one DTG cervical cancer. Both HPV16 and DTG cancers exhibited heterogeneity in $CD31^+$ vascular density from different regions of the same cancers (compare **A** with **B** and **C** with **D**). **Arrows**, $CD31^+$ vasculature. Scale bars = 200 μm.

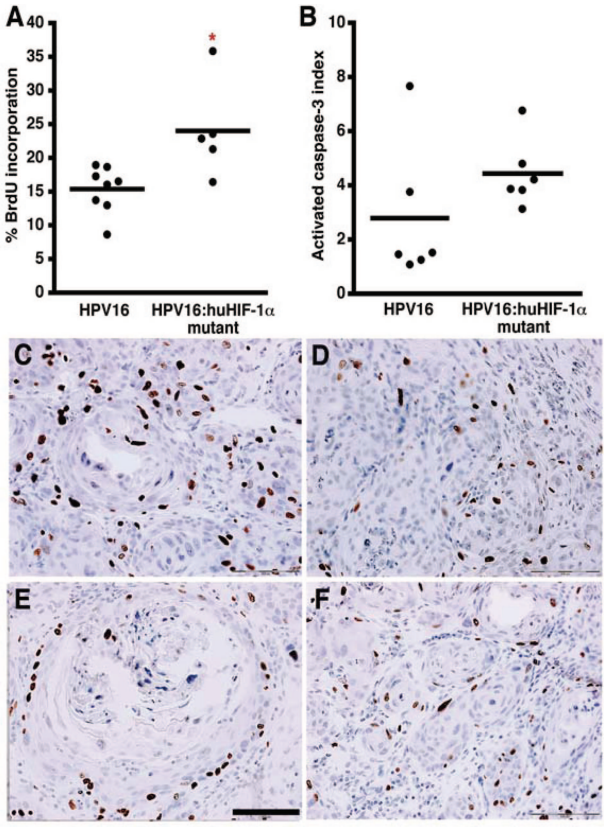

Figure 3. DNA synthesis and apoptosis in HPV16 and DTG cervical cancers. **A:** Mean BrdU index in the HPV16 mice was 15.4% compared with 24.0% in DTG mice ($P < 0.02$). **B:** Mean activated caspase-3 index in the HPV16 mice was 2.79 versus 4.44% in the DTG animals ($P = 0.093$). **C–F:** Marked variability was evident in percentage of BrdU incorporation in double- (**C** and **D**) versus single-transgenic mice (**E** and **F**). Clustered BrdU-positive cells were often seen in poorly differentiated regions, and scattered BrdU-positive nuclei in well-differentiated regions. Scale bar = 100 μm.

nohistochemical analysis also revealed a similar level of CD31-positive vasculature between massive DTG (Figure 2, C and D) and HPV16 cancers (Figure 2, A and B). Consistent with these observations, there was also a lack of differential VEGF up-regulation in DTG high-grade cervical dysplasia versus HPV16 counterparts (Figure 6C). Together, these data suggested that increased DTG cervical cancer size was not facilitated by HIF-1-mediated angiogenesis.[23]

Proliferation and Apoptosis in DTG and HPV16 Cervical Carcinomas

One mechanism for increased DTG cervical cancer size could be enhanced proliferation. Although the BrdU incorporation was relatively uniform in the HPV16 cancers (Figure 3, E and F), the index exhibited marked heterogeneity both within and between different DTG cancers (Figure 3, C and D). As such, regions with the greatest number of BrdU-labeled cells were chosen for counting by an observer blinded to the genotype. As shown in Figure 3A, the mean BrdU incorporation index of the DTG mice was 24.0 ± 3.2% compared with 15.4 ± 1.2% in HPV16 mice ($P < 0.02$). Collectively, the 9% differential proliferation rate, given persistence throughout time, could in part underlie the enhanced growth of the DTG cancers.

Immunohistochemical analysis of caspase-3 activation in cancers from single and double-transgenic mice was also challenging because the keratin pearls or less well-differentiated malignant squamous aggregates had central regions filled with cells and cellular debris that were positive for activated caspase-3 (data not shown). These regions were not included in the analysis. Instead, we focused on basaloid and suprabasal malignant cells at the epithelial-stromal interface for apoptotic index quantification. As shown in Figure 3B, there was a trend toward increased apoptosis in the DTG cancers (4.44 ± 0.52%) when compared with the HPV16 cancers (2.79 ± 1.06%) ($P = 0.093$). Expression of the proapoptotic BH3-only domain protein BNIP3 was also differentially (but not significantly) elevated, in double- versus single-transgenic mice (Figure 6D). Borderline low-level induction of apoptosis in DTG mice was obviously insufficient to compensate for the increased proliferation in DTG cancers. Thus, the differential between proliferation and apoptosis could explain, in part, the massive size of the cervical cancers in the DTG mice.

Genome-Wide Transcriptional Expression Analyses of Cervices and Upper Vagina Derived from 3-Month Estrogen-Treated Nontransgenic, HPV16, HIF-1 Mutant, and DTG Mice

Although our biological data were compelling, we strove to determine the molecular underpinnings of the HPV16 and HIF-1 combinatorial induction of advanced local cervical cancer. To facilitate identification of a disease progression signature transcriptome, we focused on global gene expression profiles in high-grade dysplasia of 3-month estrogen-treated transgenic mice (a stage consisting predominantly of CINIII, rarely carcinoma *in situ* but no invasive malignancy).[22] We used total RNA derived from the entire cervix in an attempt to determine both cell autonomous changes in epithelial genes as well as non-cell autonomous changes in stromal cell-specific genes. First, we focused on validation of the HPV16 transgenic model by identifying HPV16 signature probe sets. We performed SAM analysis on the array dataset using a stringency parameter with a twofold-change cutoff and a 0.01% mean false discovery rate. SAM analysis revealed statistically significant alterations in a total of 107 probe sets (Figure 4). The microarrays also demonstrated a striking up-regulation of nearly the complete gene repertoire controlled by the E2F transcription factor,[25,26] which is itself negatively regulated by the retinoblastoma protein (pRB). As pRB is sequestered and destabilized by HPV16 E7 oncoprotein, E2F is activated.[27,28] The differentially expressed E2F targets in the estrogen-treated K14-HPV16 transgenic dysplastic cervices included genes regulating nucleotide synthesis, thymidine kinase, dihydrofolate reductase, ribonuclease reductase M2, cell cycle

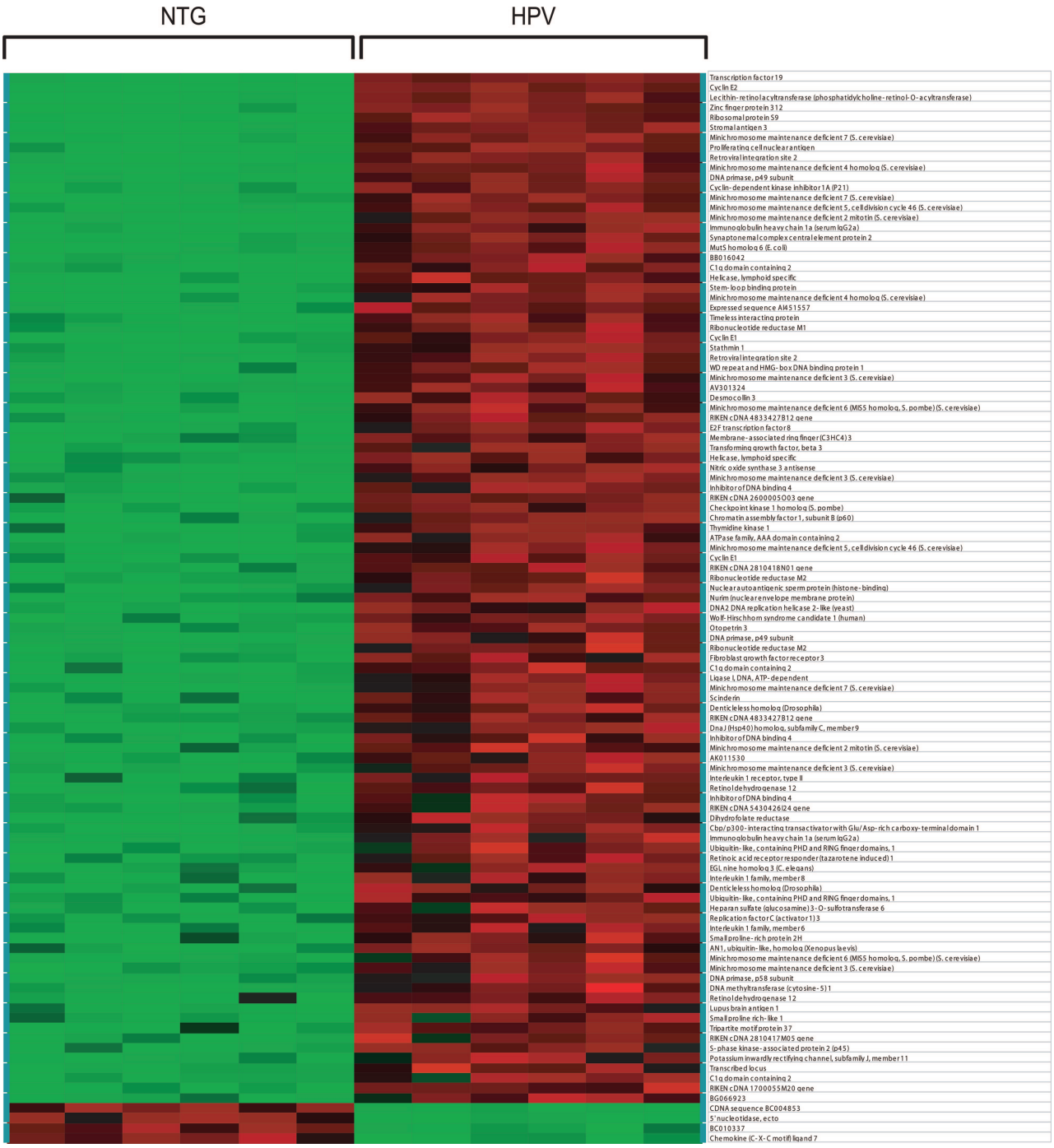

Figure 4. Expression of HPV16-regulated genes in cervices and upper vagina from 3-month estrogen treated nontransgenic and HPV16 transgenic mice. Heat maps of the normalized *z*-scores of hybridization signals of selected probe sets by nontransgenic and HPV16 genotypes. All listed probe sets exhibited significant differences in gene chip signal intensities between nontransgenic and HPV16 samples according to statistical analysis of microarray (SAM) analysis.

progression, cyclin E1 and E2, and DNA synthesis, DNA polymerase, DNA helicases and primases, minichromosome maintenance genes, and proliferating cell nuclear antigen.[25,26]

After determination of the transcriptome in the dysplastic K14-HPV16 cervix, we next determined whether the HPV16 and HIF-1α combination produced a unique global clustering of dysregulated genes. This analysis compared total RNA samples from DTG, HPV16, and nontransgenic cervices (Figure 5C). Unsupervised hierarchical clustering analysis of the 32,740 expressed probe sets (see Materials and Methods) resulted in a striking partitioning of each genotype (Figure 5C). HPV16 and nontransgenic gene expression patterns were tightly segregated into two distinct groups, whereas the DTG cancers exhibited a markedly heterogeneous partitioning pattern but still segregated away from both the nontransgenic and HPV16 cluster groups (Figure 5C). This heter-

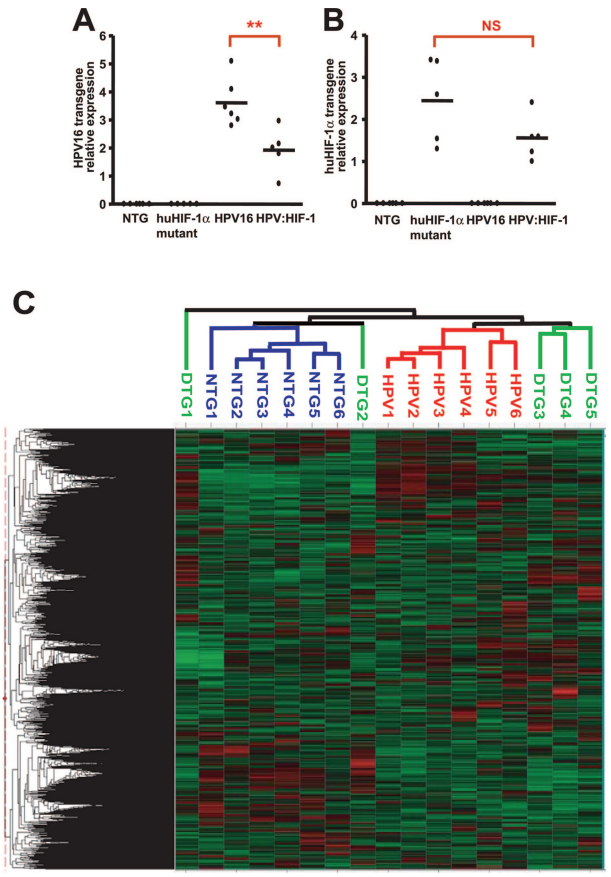

Figure 5. Microarray analyses of global gene expression in cervices and upper vagina derived from 3-month estrogen-treated nontransgenic, HPV16, and DTG mice. **A** and **B:** Quantitative real-time RT-PCR analysis of transgene expression. Expression of either HPV16 (**A**) or constitutive HIF-1 mutants (**B**) was lower in the double- compared with single-transgenic mice (**$P < 0.01$, Student's *t*-test). **C:** Unsupervised hierarchical clustering analysis of the 32,740 expressed Affymetrix microarray probe sets resulted in the striking segregation of two distinct groups according to nontransgenic (shown in blue color) versus HPV16 transgenic (red) genotype. Five DTG cancers (green) displayed marked heterogeneity in their partitioning patterns, with three samples forming a separate cluster group and the remainder segregated away from all three cluster groups.

ogeneity of global gene expression in the DTG mice is intriguing in light of the differential cancer progression seen in these mice treated with the longer, 6-month estrogen regimen. Remarkably, only 21 of 107 HPV16 probe sets exhibited significant alterations in DTG samples, when compared with the single HPV16 transgenic samples ($P < 0.04$ by *t*-tests) (Figure 6, A and B), suggesting that HIF-1 (and/or its noncanonical targets) can functionally regulate HPV16 oncogene activities in dysplastic cervices. A HPV16 oncogene and HIF-1 target gene global genetic interaction was also validated by subsequent real-time RT-PCR analysis. First, the HPV16 or the HIF-1α transgenes were lower in the DTG mice compared with their respective single-transgenic counterparts (Figure 5, A and B). Second, many HIF-1 targets, including VEGF, BNIP3, IGF-BP3, transforming growth factor (TGF)-α, carbonic anhydrase IX (CAIX), CXCR4, COX2, and uPAR, although overexpressed in single K14-HIF-1α transgenic cervices were not differentially up-regulated in DTG versus HPV16 dysplasia cervices (Figure 6, C–J; Table 2 for a full list), with the notable exception of carbonic anhydrase IX (Figure 6G). These data supported the hypothesis that HPV16 viral genome interferes at some level with the HIF-1 target gene expression in dysplastic cervices. Consistent with this hypothesis, K14-HPV16 single transgenic cervices also evidenced down-regulation of several HIF-1 targets including CAIX, CXCR4, and uPAR (Figure 6, G, I, and J; compare HPV16 with NTG). Taken together, these results provided clear evidence that HPV16 oncogenes and HIF-1 gain of function reciprocally regulate the expression of a subset of each other's canonical target genes in DTG dysplasia cervices, suggesting that the two factors functionally interact at a level yet to be determined.

Genome-Wide Transcriptional Expression Analyses of DTG versus HPV16 High-Grade Premalignant Cervices

Determination of the HPV16 and DTG transcriptome and genetic interaction set the stage for an analysis of the global genetic networks potentially responsible for promoting differential DTG cervical cancer growth. SAM analysis comparing HPV16 and DTG samples (Figure 7A) using a stringency parameter with a twofold-change cutoff and a 6.3% mean false discovery rate revealed statistically significant alterations in 101 probe sets (Figure 7B). As shown in Figure 7C, 69 mRNAs consistently showed an increase in expression levels, and 32 mRNAs showed a reduction by greater than twofold. We further identified an additional 1104 statistically significant probe sets, 618 genes up-regulated and 486 down-regulated, between double- versus single-transgenic samples based on a 1.5-fold but less than twofold change (Supplemental Table 2, see *http://ajp.amjpathol.org*). We next performed gene ontology (GO) analysis to map the specific biological processes (and molecular functions) in which the significant genes play a role. Several major biological pathways were either up- or down-regulated in DTG compared with single transgenic cervices (Figure 7, D–G). Genes expressed at higher levels in DTG cervices included growth factors and signal transducers (Figure 7D, $P = 0.0045$), several genes within the cytoskeleton, cell morphology, and adhesion categories (Figure 7E, $P = 0.031$), peptidases/proteases (Figure 7F, $P = 0.039$), other C-N bond hydrolases (data not shown), and inflammatory and wound response mediators (Figure 7G, $P < 0.0001$). Genes differentially expressed at lower levels in DTG cervices included several epithelial-specific cytoskeleton, cell morphology, and adhesion genes (Figure 7E, $P = 0.031$), and several protease inhibitors (Figure 7F).

Next, RT-PCR analysis was undertaken to validate selected genes from the microarray study as well as candidate genes of which up- or down-regulation is associated with human cervical cancer progression (Figure 8 and Table 2). Analysis of candidate genes from the microarray experiments confirmed the up-regulation of Ceacam1, rhophilin, CXCL7, and Adam8 (Figure 8, A–D), along with reductions in loricrin, desmocollin 1, and desmoglein 1α (Figure 8, G–I). Of clinical relevance was the

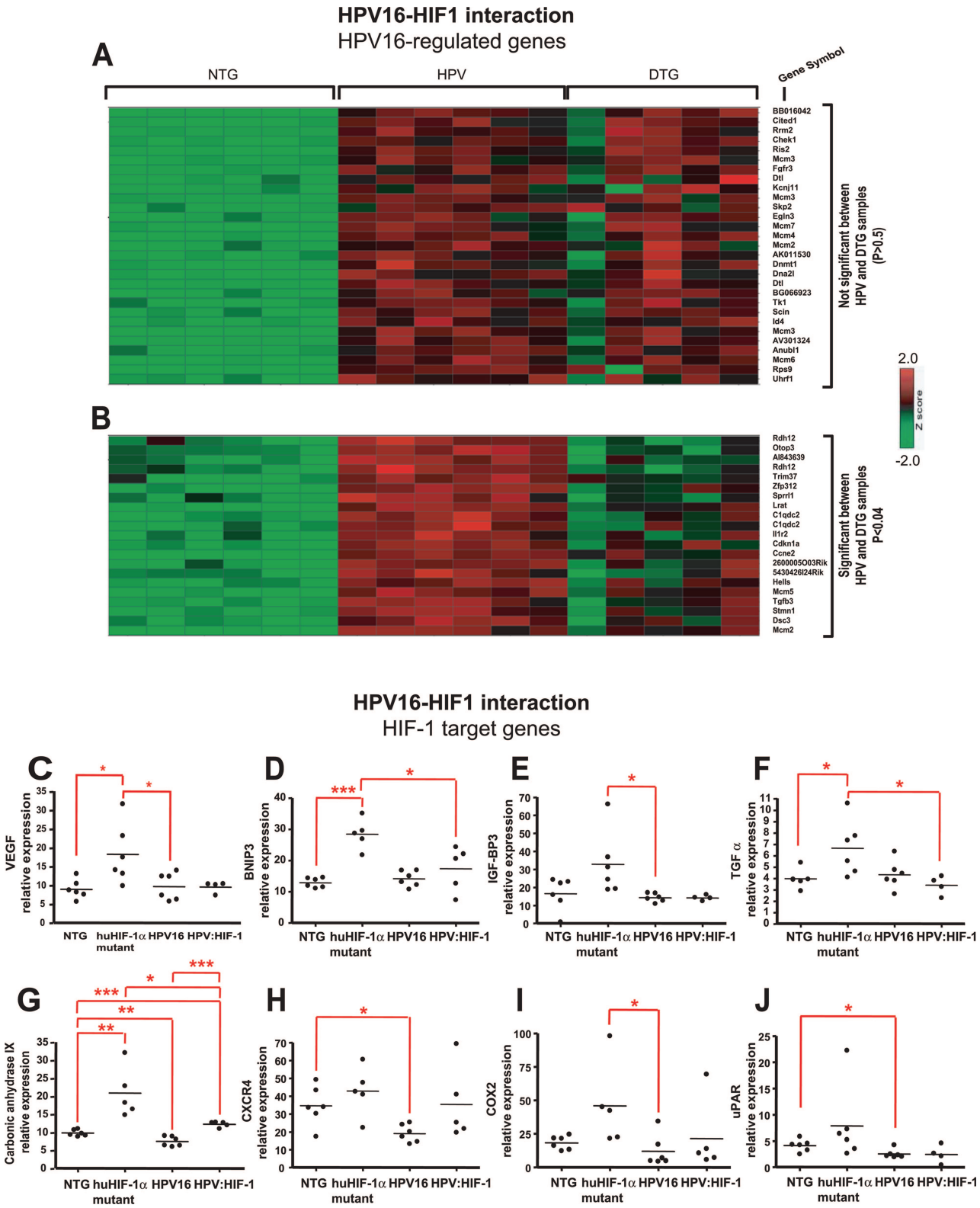

Figure 6. Expression of HPV16-regulated and HIF-1 target genes in cervices and upper vagina from 3-month estrogen-treated nontransgenic, HPV16, HIF-1 mutant, and DTG mice. **A** and **B:** Heat maps of normalized *z*-scores of hybridization signals of selected probe sets by nontransgenic, HPV16, and DTG genotypes. All listed probe sets exhibited significant differences in gene chip signal intensities between nontransgenic and HPV16 samples according to statistical analysis of microarray (SAM) analysis. **B:** Twenty-one probe sets exhibited significant alterations in DTG samples when compared with the HPV16 samples ($P < 0.04$ by *t*-tests). The gene symbol for each probe set is listed on the right side. **C–J:** Real-time RT-PCR analysis of HIF-1 target gene expression including VEGF, BNIP3, IGF-BP3, TGF-α, CAIX, CXCR4, COX2, and uPAR (*$P < 0.05$, **$P < 0.01$, ***$P < 0.001$; Student's *t*-test).

Table 2. RT-PCR Candidate Gene Analysis

Gene	Relative expression difference* (*P* value)
Desmocollin 1	Decreased (<0.0001)
Desmoglein 1α	Decreased (<0.001)
Ceacam1	Increased (<0.0001)
Rhophilin	Increased (<0.001)
Adam8	Increased (<0.05)
Loricrin	Decreased (<0.001)
Carbonic anhydrase IX	Increased (<0.05)
Mucin1	NS
Ghrelin	NS
BNIP3	NS
Adrenomedullin	NS
IGFBP3	NS
COX2	NS
c-Met	NS
CXCR4	NS
Cyclin D1	NS
Cyclin E	Decreased (<0.001)
Erythropoietin	NS
Erythropoietin receptor	NS
Glut-1	NS
Hes1	NS
Hes5	NS
Hey1	Decreased (<0.001)
IGF2	NS
IL-1α	Increased (<0.05)
MIP2	NS
Notch1	Decreased (<0.05)
P65	NS
SDF-1	NS
TGF-α	NS
TNF-α	Increased (<0.05)
uPAR	NS
VEGF	NS
Mmp2	NS
Mmp9	NS

NS, not significant.
*Relative expression difference between double transgenics and K14-HPV16.

confirmed differential up-regulation of chemokines and cytokines known to be overexpressed in human cervical cancers, including interleukin (IL)-1 ($P < 0.05$) (Figure 8E) and tumor necrosis factor (TNF)-α ($P < 0.05$) (Figure 8F) in the DTG mice. Collectively, both the microarray and the RT-PCR data provided evidence that HIF-1 and HPV16 oncogenes recruit a unique genetic network in mouse premalignant cervices. In addition, both analyses also suggested that many HIF-1 canonical targets were not induced at the premalignant stage in the context of HIF-1α-HPV16 coexpression.

Cross-Examination of DTG Signature Transcriptome and HIF-1 Target Gene Expression in Human Normal and Malignant Cervices

To determine whether our DTG gene expression signature contained markers predictive for human cervical cancer progression, the DTG microarray dataset was interrogated for matching probe sets to a publicly available cDNA microarray dataset derived from staged human cervical cancers and normal cervices (Gene Expression Omnibus GDS470 dataset on a GPL355 human 10K array).[29] Specifically, this dataset contains expression profiles of eight normal cervical samples and 24 cervical cancers at stages IB, IIA, IIB, and IIIB of the FIGO system.[30] Our DTG transgenic mouse dataset contained 60 human orthologue genes. One-way analysis of variance revealed 15 of these human genes with altered expression among the normal, stage IB, and stage II (IIA and IIB) of cervical cancer ($P < 0.05$). Eight of the 15 genes displayed differential expression patterns consistent with progression between stage IB and stage II (Figure 9A). These include RNASE1, MMP7, IGFBP1, MUC1, PIK3CD, LIF, STAT2, and CLCA2. Thus, a subset of differentially expressed genes in mouse DTG premalignant cervices also predicts progression of human cervical cancer. Collectively, these data provided evidence that the combination of HPV16 oncogene expression with HIF-1 downstream signaling components coordinated a unique downstream molecular network setting the stage for the ultimate elaboration of aggressive, advanced cervix cancer across species.

In light of our observations that expression of many HIF-1 canonical targets was suppressed in premalignant cervices of the DTG mice, we were motivated to perform a cross-species comparison of HIF-1 targets in the human cervical cancer microarray data. We identified HIF-1α itself and 27 HIF-1 target genes as being present on both the mouse and human array platforms. Multiple *t*-test analyses revealed that VEGF, HK1, EPO, c-MET, and IGFBP2 genes were up-regulated, and COL5A1 (collagen type 5 α1) was down-regulated in malignant versus normal cervices ($P < 0.05$) (Figure 9B). In addition, TGF-β1, TGF-β3, and IGFBP3 mRNAs exhibited an increased abundance, and c-MET a reduced level, in stages IIA, IIB, and IIIB versus stage IB of cancer ($P < 0.05$). The expression of adrenomedullin, a gene regulating angiogenesis seemed to be mildly reduced during stage IB and up-regulated with progression to stage II ($P < 0.03$). Principal component analysis with the 10 significant HIF-1 target genes revealed a high-level partitioning of normal cervices, stage IB cancers, and stages II and III cancers (Figure 9C). Although these data seem to contradict the HIF-1 target gene down-regulation presented in Figure 6, the entry point of the two studies are different; our analysis is of high-grade dysplasia, and the human data are derived from sampling cancers. In fact, novel mechanistic inferences can be postulated from this cross-species analysis as detailed below.

Discussion

In the present work, we used a DTG cervical cancer model developed by our group[21–23] to test the role of HIF-1α gain of function in pathogenesis of the disease. Expression of either of two constitutively active HIF-1α mutants produced a massive increase in cancer growth and invasiveness that was independent of VEGF expression and of alterations in tumor microvascularity. The effect of HIF-1α gain of function was specific for local growth because neither cancer incidence nor metastasis

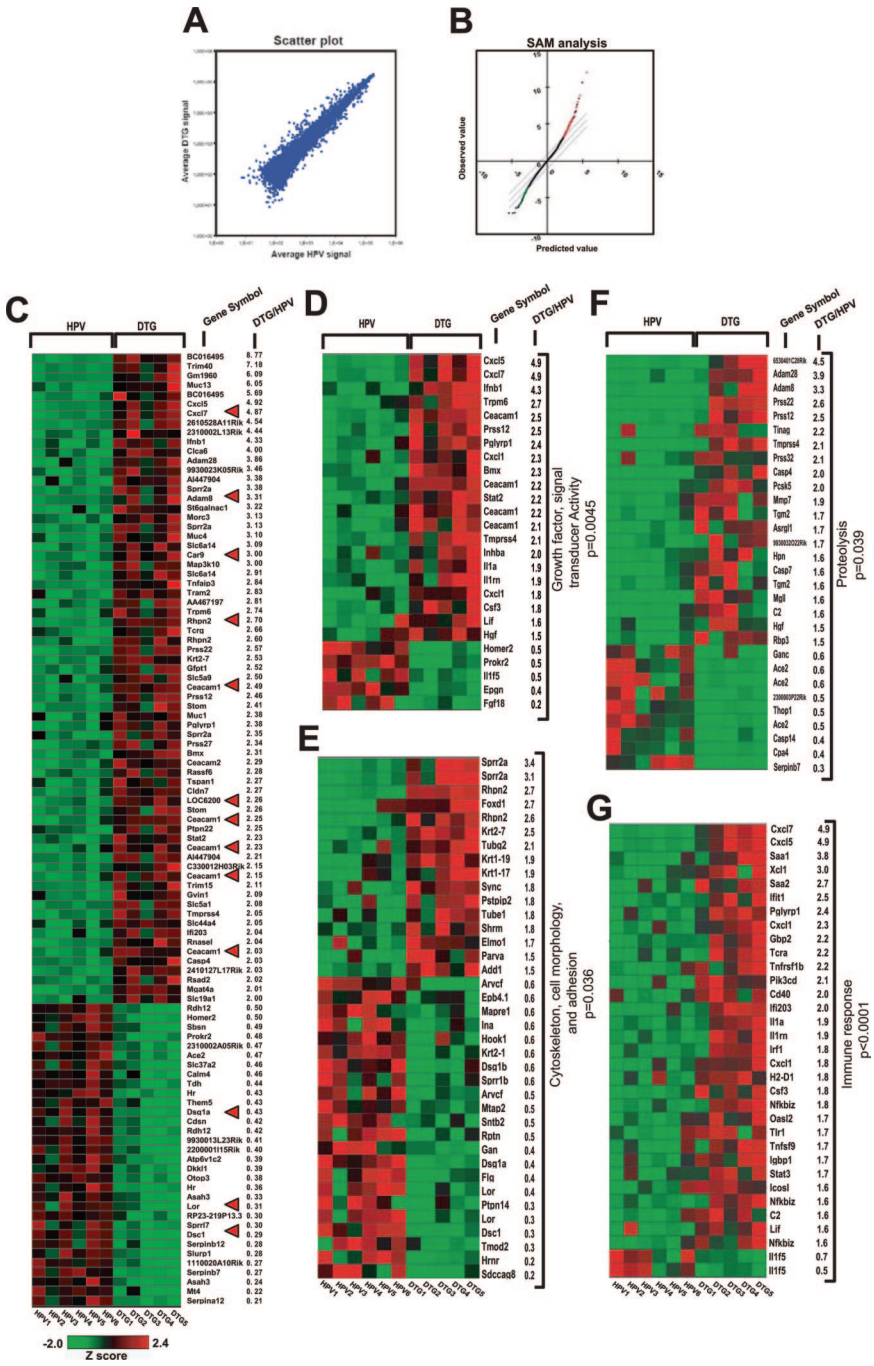

Figure 7. Microarray analyses of global gene expression in high-grade dysplastic cervices of double- versus single-transgenic mice. **A:** Log10 scatter plot of the average gene chip hybridization signal intensity for each probe set of the HPV16 samples ($n = 6$) on the x axis versus the average DTG signal ($n = 5$) on the y axis. **B:** Results from SAM analysis of the expressed dataset. Spots in green and red represent a total of 101 probe sets that are significantly altered in DTG samples compared with HPV16 single transgenic levels. **C:** Heat map of normalized z-scores of the hybridization signals of the 101 significant probe sets. The gene symbol and fold of change between double- and single-transgenic samples for each probe set are listed on the right side. **Red triangles** mark the probe sets where altered transcriptional expression of the corresponding genes has been confirmed with quantitative RT-PCR analysis (shown in **D–G**). **D–G:** Gene Ontology (GO) mapping of differentially displayed genes into molecular function and biological process categories. Significant probe sets by SAM analysis and those by simple unpaired t-tests (1.5-fold change cutoff and $P < 0.05$) were combined (1104 probe sets), and subjected to the GO analysis using the Spotfire DecisionSite program. Heat-maps of z-score-normalized hybridization signals of the significant probe sets were present by the GO categories: growth factors and signal transducers (**D**); cell cytoskeleton, morphology, adhesion, and differentiation (**E**); proteases and regulators of proteolysis (**F**); genes encoding factors mediating immune (inflammatory/wound) responses (**G**). The gene symbol and fold change between double- and single-transgenic samples for each probe set are listed on the right side.

was affected. Transcriptional profiling and real-time RT-PCR analysis of DTG high-grade dysplastic cervices demonstrated that the combination of HPV oncoproteins and constitutively active HIF-1α regulated both direct (canonical) HIF-1 targets and multiple indirect gene networks, ultimately creating a distinct molecular milieu in premalignant cervical epithelium and stroma that fostered advanced cervix cancer.

Our data highlighted differentially increased proliferation compared with apoptosis as being responsible, in part, for the markedly increased tumor size in DTG cervical cancers. The proposed function of HIF-1α in proliferation in the literature is conflicting, presumably because of cell-type and/or experimental condition differences. Hypoxia-induced HIF-1α was reported to mediate cell-cycle arrest in mouse embryonic stem cells.[31] Release of glucose deprivation depressed HIF-1α levels in these ES cells, stimulated mitosis, and promoted proliferation.[32,33] In contrast, constitutive expression of HIF-1α enhanced cellular proliferation in other cell contexts.[32] In this regard, many canonical HIF-1 targets (listed in Table 2) are widely believed to be the mediators of cell proliferation and tumor progression.[34] Surprisingly, we discovered that a number of these HIF-1 targets were not induced in DTG premalignant cervices. In contrast, indirect genetic networks were up-regulated in DTG cervices that could have contributed to the emergence

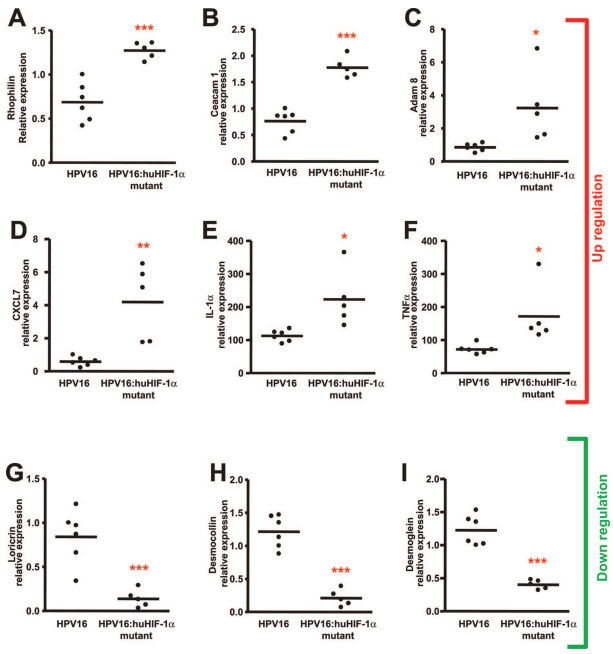

Figure 8. Real-time RT-PCR analysis of gene expression in high-grade dysplastic cervices of DTG versus HPV16 mice. **A–F:** Statistically significant differential elevations of the rhophilin, Ceacam1, Adam8, CXCL7, IL-1, and TNF-α were evident in the double- compared with single-transgenic mice. **G–I:** Significant decreases were detected in the transcripts encoding differentiation and adhesion molecules loricrin, desmocollin, and desmoglein ($^{*}P < 0.05$, $^{**}P < 0.01$, $^{***}P < 0.001$; Student's *t*-test).

of massive malignancies (see below). There are also conflicting reports on HIF-1's role in apoptosis. Although HIF-1α was required for apoptosis in tumor allografts of HIF-1α knockout ES cells, HIF-1α was dispensable for hypoxia-induced apoptosis of mouse ES cells and human malignant cell lines in cell culture.[35,36] At the molecular level, HIF-1 has been shown to induce transcription of the proapoptotic BH3 domain protein BNIP3. However, the role of BNIP3 in hypoxia/anoxia-mediated apoptosis is cell-type- and experiment-context-dependent as well.[9] HIF-1 has also been shown to facilitate apoptosis by stabilization of p53.[35,36] However, p53 expression is undetectable in this transgenic cervical cancer model[22] because of HPV16 E6 oncoprotein-mediated polyubiquitylation and proteasomal degradation.[37] Thus, lack of p53 function, in conjunction with insufficient BNIP3 up-regulation (Figure 6F), may explain, in part, the lack of compensatory apoptosis in face of enhanced DTG proliferation.

Although increased proliferation led to massive cervical cancers in DTG mice, this effect was not uniformly detected. Among several possible explanations for the apparent bimodal distribution of tumor sizes in the DTG mice, we favor the notion that additional rate-limiting molecular events may dictate the latency of progression. As such, longer experimental time intervals will be required to determine the ultimate penetrance of massive cervical malignancies in DTG mice. Our microarray analysis also mirrored the DTG cancer size heterogeneity by segregating in a bimodal partitioning pattern (Figure 5A). As such, three of five of DTG samples were clustered into a distinct group whereas the remaining samples were disparate, one was a unique cluster distinct from either the other DTG or HPV groups, whereas the other DTG sample was closely related to the nontransgenic cluster. This heterogeneity of global gene expression in the DTG mice may represent the molecular underpinnings for the differential cancer progression seen in these mice. In addition, individual variability of estrogen-responsiveness in the DTG mice or the cervical target tissue may have contributed to cancer size heterogeneity. Despite the DTG size and global gene expression heterogeneity, it is striking that only a few gene markers derived from these mice predicted cervical cancer progression in humans, where small sample size and genetic heterogeneity was paramount (Figure 9A). These molecular data also bolstered the clinical relevance of the DTG mouse as a model of advanced cervical cancer.

Our work represents the first functional genomics study of the mouse model of cervical cancer in comparison to human disease. Microarray analysis of HPV16 single transgenic cervices identified a myriad of HPV16 signature target genes (Figure 4), including downstream E2F targets[25,26] that were the result of pRB destabilization by HPV16 E7.[28] Up-regulation of several minichromosome maintenance genes, including minichromosome maintenance genes 2 to 7, is particularly interesting because these proteins, regulators of formation and progression of the DNA replication complex, are also markers of progression of high-grade human cervical dysplasias to cancer.[38–40] These results were dual validation of both the estrogen-treated K14-HPV16 transgenic mice as models of human cervical carcinogenesis, and our approach of using total RNA isolated from the entire cervix to detect both epithelial and stromal gene expression alterations.

Our extensive expression analysis also provided mechanistic insights into the role of HIF-1 in cell growth and invasion of cancers. Our results suggested a mechanism whereby growth, proliferation, and invasion could be enhanced in DTG cervices by expression changes in mRNAs encoding molecules that mediate cross talk between the epithelium and stroma. First, the differential increase in chemokines and cytokines including TNF-α, IL-1, CXCL1, CXCL5, CXCL7, and interferon-induced protein B gene expression could provide both a cell autonomous and paracrine stimulus for differential growth. A number of studies demonstrated that both TNF-α and IL-1 increased in clinical high-grade dysplasia and cervical cancer.[41] TNF-α-mediated apoptosis and growth arrest of genital keratinocytes was obviated by transfection of HPV E6 and E7 oncoproteins.[42,43] TNF-α stimulated proliferation of HPV16 E6 and E7 expressing genital keratinocytes secondary to expression of both viral oncogene mRNA stabilization and induction of EGFR signaling via amphiregulin up-regulation.[44] Other pathways for which HPV and HIF-1 combinatorial transcriptome modulation could affect cancer behavior were alterations in expression of genes controlling adhesion, cell migration, and differentiation. In particular, coordinate up-regulation of rhophilin concomitant with desmoglein and desmocollin down-regulation suggested a mechanism whereby Rho sequestration could produce a more invasive phenotype by actin depolymerization and pseu-

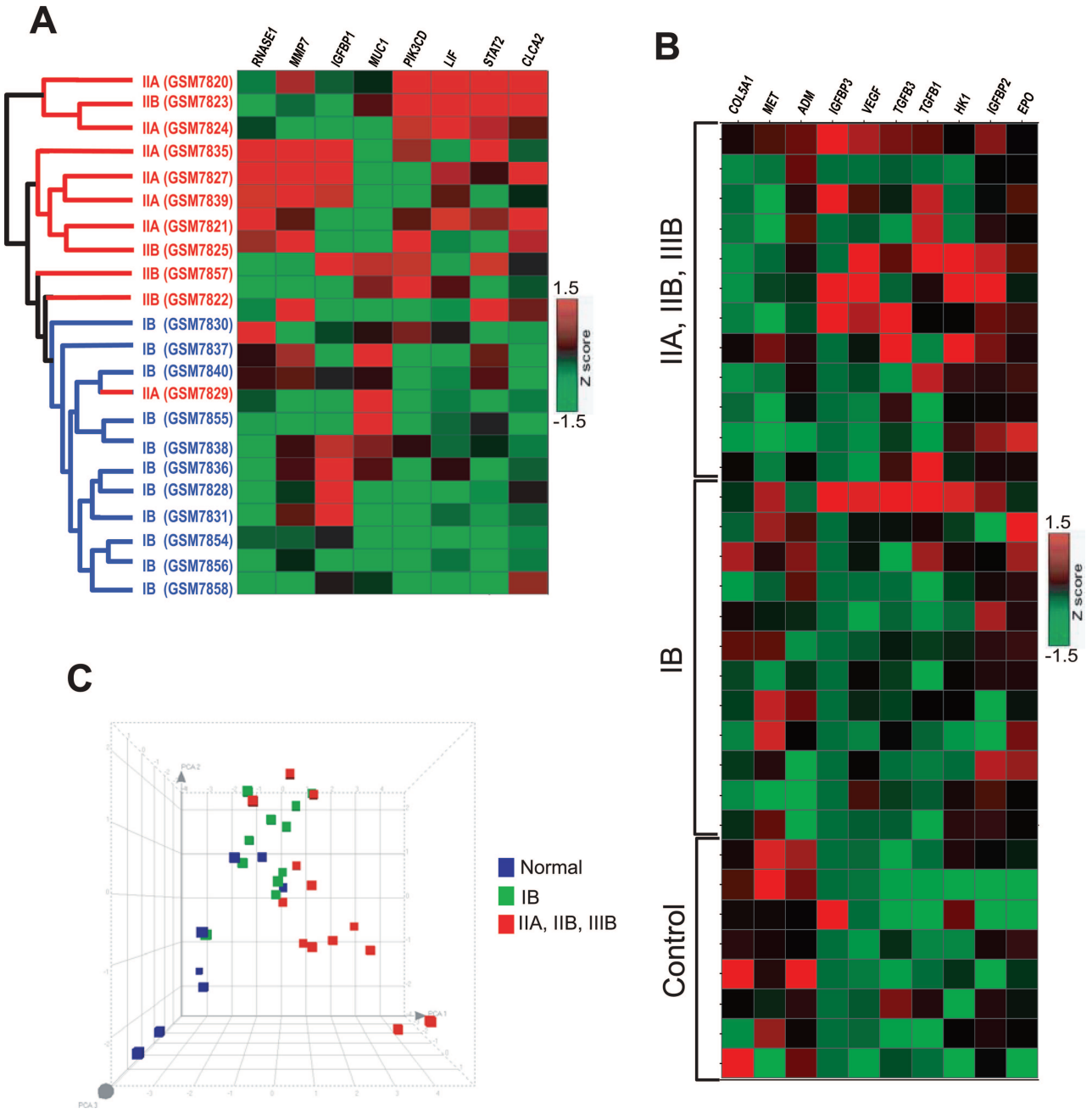

Figure 9. Cross-examination of transcriptional expression of DTG signature and HIF-1 target genes in different stages of human malignant cervices. **A:** Unsupervised hierarchical clustering analysis of eight DTG signature genes resulted in striking partitioning of stage II (IIA and IIB) cervical cancers (shown in red color) from stage IB cancers (blue) ($P < 0.05$). **B:** Heat map of normalized *z*-scores of hybridization signals of 10 selected HIF-1 target genes grouped according to disease stage (normal, stage IB, stage IIA, stage IIB and stage IIIB). **C:** Principal component analysis of 32 cervical samples based on 10 selected HIF-1 target genes resulted in a partitioning of normal, stage IB, and stages II and III samples.

dopodia protrusion,[45,46] along with decreased cell-cell adhesion (Mmp7, Adam8, Adam28, and Tmprss4). Reduction in loricrin levels was also consistent with decreased terminal differentiation and a more immature squamous cell phenotype, and correlated with regions of dedifferentiation detected in the double- compared with single-transgenic cervical cancers.

However, the relative paucity of direct HIF-1 transcriptional targets in our DTG signature transcriptome seemed at face value to be at odds with our supervised clustering of advanced human cervical cancers based on these directly regulated HIF-1 genes. Sampling from different stages of premalignant or malignant disease is one explanation. The other mechanistic explanation is that the HPV-HIF-1 transcriptome could provide the molecular milieu that propels those dysplasias with gain of HIF-1 function to advanced cervical cancer. Once these large malignancies are established, microenvironmental heterogeneity characterized by acidotic and hypoxic regions could be the stimuli for further HIF-1 up-regulation that then up-regulates the direct and canonical targets of the transcription factor. Microenvironmental heterogeneity in advanced cancers could also be

responsible for genomic instability[5] that in turn may coordinate phenotypes not seen in the transgenic model, such as metastasis. Consistent with the latter notion, a HIF-1 function in metastasis has recently been identified in a human breast cancer xenograft model.[47]

In summary, we determined that combinatorial HPV16 oncogene expression and HIF-1α gain of function produced locally advanced cervical cancers closely emulating the histopathological features of advanced local clinical disease. A distinct repertoire of predominantly indirect downstream genetic networks was activated in HPV16-HIF-1α mutant DTG mice that facilitated emergence of advanced cervical cancer. Regulation of multiple genetic networks by the combination of HPV16 viral oncogenes and HIF-1 suggests a novel noncanonical mechanism for functional interaction(s) of this master regulatory transcription factor with environmental or endogenous initiators of carcinogenesis.

Acknowledgments

We thank Drs. Timothy J. Ley, Loren Michel, Jason Weber, and Jeffrey Milbrandt for comments on the manuscript; Katie Manning for technical assistance; and Michelle Noll for animal husbandry.

References

1. Walboomers JM, Jacobs MV, Manos MM, Bosch FX, Kummer JA, Shah KV, Snijders PJ, Peto J, Meijer CJ, Munoz N: Human papillomavirus is a necessary cause of invasive cervical cancer worldwide. J Pathol 1999, 189:12–19
2. Lowy DR, Schiller JT: Prophylactic human papillomavirus vaccines. J Clin Invest 2006, 116:1167–1173
3. Hockel M, Schlenger K, Aral B, Mitze M, Schaffer U, Vaupel P: Association between tumor hypoxia and malignant progression in advanced cancer of the uterine cervix. Cancer Res 1996, 56:4509–4515
4. Dehdashti F, Grigsby PW, Mintun MA, Lewis JS, Siegel BA, Welch MJ: Assessing tumor hypoxia in cervical cancer by positron emission tomography with 60Cu-ATSM: relationship to therapeutic response—a preliminary report. Int J Radiat Oncol Biol Phys 2003, 55:1233–1238
5. Graeber TG, Osmanian C, Jacks T, Housman DE, Koch CJ, Lowe SW, Giaccia AJ: Hypoxia-mediated selection of cells with diminished apoptotic potential in solid tumours. Nature 1996, 379:88–91
6. Vaupel P, Kelleher DK, Hockel M: Oxygen status of malignant tumors: pathogenesis of hypoxia and significance for tumor therapy. Semin Oncol 2001, 28(Suppl 8):S29–S35
7. Chi JH, Knudson MM, Vassar MJ, McCarthy MC, Shapiro MB, Mallet S, Holcroft JJ, Moncrief H, Noble J, Wisner D, Kaups KL, Bennick LD, Manley GT: Prehospital hypoxia affects outcome in patients with traumatic brain injury: a prospective multicenter study. J Trauma 2006, 61:1134–1141
8. Semenza GL: Targeting HIF-1 for cancer therapy. Nat Rev Cancer 2003, 3:721–732
9. Erler JT, Bennewith KL, Nicolau M, Dornhofer N, Kong C, Le QT, Chi JT, Jeffrey SS, Giaccia AJ: Lysyl oxidase is essential for hypoxia-induced metastasis. Nature 2006, 440:1222–1226
10. Mole DR, Pugh CW, Ratcliffe PJ, Maxwell PH: Regulation of the HIF pathway: enzymatic hydroxylation of a conserved prolyl residue in hypoxia-inducible factor α subunits governs capture by the pVHL E3 ubiquitin ligase complex. Adv Enzyme Regul 2002, 42:333–347
11. Bae SH, Jeong JW, Park JA, Kim SH, Bae MK, Choi SJ, Kim KW: Sumoylation increases HIF-1α stability and its transcriptional activity. Biochem Biophys Res Commun 2004, 324:394–400
12. Min JH, Yang H, Ivan M, Gertler F, Kaelin Jr WG, Pavletich NP: Structure of an HIF-1α-pVHL complex: hydroxyproline recognition in signaling. Science 2002, 296:1886–1889
13. Thomas GV, Tran C, Mellinghoff IK, Welsbie DS, Chan E, Fueger B, Czernin J, Sawyers CL: Hypoxia-inducible factor determines sensitivity to inhibitors of mTOR in kidney cancer. Nat Med 2006, 12:122–127
14. Richard DE, Berra E, Gothie E, Roux D, Pouyssegur J: p42/p44 mitogen-activated protein kinases phosphorylate hypoxia-inducible factor 1alpha (HIF-1α) and enhance the transcriptional activity of HIF-1. J Biol Chem 1999, 274:32631–32637
15. Sang N, Stiehl DP, Bohensky J, Leshchinsky I, Srinivas V, Caro J: MAPK signaling up-regulates the activity of hypoxia-inducible factors by its effects on p300. J Biol Chem 2003, 278:14013–14019
16. Mekhail K, Gunaratnam L, Bonicalzi ME, Lee S: HIF activation by pH-dependent nucleolar sequestration of VHL. Nat Cell Biol 2004, 6:642–647
17. Birner P, Schindl M, Obermair A, Plank C, Breitenecker G, Oberhuber G: Overexpression of hypoxia-inducible factor 1α is a marker for an unfavorable prognosis in early-stage invasive cervical cancer. Cancer Res 2000, 60:4693–4696
18. Bachtiary B, Schindl M, Potter R, Dreier B, Knocke TH, Hainfellner JA, Horvat R, Birner P: Overexpression of hypoxia-inducible factor 1α indicates diminished response to radiotherapy and unfavorable prognosis in patients receiving radical radiotherapy for cervical cancer. Clin Cancer Res 2003, 9:2234–2240
19. Maxwell PH, Dachs GU, Gleadle JM, Nicholls LG, Harris AL, Stratford IJ, Hankinson O, Pugh CW, Ratcliffe PJ: Hypoxia-inducible factor-1 modulates gene expression in solid tumors and influences both angiogenesis and tumor growth. Proc Natl Acad Sci USA 1997, 94:8104–8109
20. Ryan H, Poloni M, McNulty W, Elson D, Gassmann M, Arbeit J, Johnson R: Hypoxia-inducible factor-1α is a positive factor in solid tumor growth. Cancer Res 2000, 60:4010–4015
21. Arbeit JM, Howley PM, Hanahan D: Chronic estrogen-induced cervical and vaginal squamous carcinogenesis in human papillomavirus type 16 transgenic mice. Proc Natl Acad Sci USA 1996, 93: 2930–2935
22. Riley RR, Duensing S, Brake T, Munger K, Lambert PF, Arbeit JM: Dissection of human papillomavirus E6 and E7 function in transgenic mouse models of cervical carcinogenesis. Cancer Res 2003, 63:4862–4871
23. Elson DA, Thurston G, Huang LE, Ginzinger DG, McDonald DM, Johnson RS, Arbeit JM: Induction of hypervascularity without leakage or inflammation in transgenic mice overexpressing hypoxia-inducible factor-1α. Genes Dev 2001, 15:2520–2532
24. Arbeit JM, Munger K, Howley PM, Hanahan D: Progressive squamous epithelial neoplasia in K14-human papillomavirus type 16 transgenic mice. J Virol 1994, 68:4358–4568
25. Polager S, Kalma Y, Berkovich E, Ginsberg D: E2Fs up-regulate expression of genes involved in DNA replication, DNA repair and mitosis. Oncogene 2002, 21:437–446
26. Black EP, Hallstrom T, Dressman HK, West M, Nevins JR: Distinctions in the specificity of E2F function revealed by gene expression signatures. Proc Natl Acad Sci USA 2005, 102:15948–15953
27. Jones DL, Thompson DA, Münger K: Destabilization of the RB tumor suppressor protein and stabilization of p53 contribute to HPV type 16 E7-induced apoptosis. Virology 1997, 239:97–107
28. Gonzalez SL, Stremlau M, He X, Basile JR, Münger K: Degradation of the retinoblastoma tumor suppressor by the human papillomavirus type 16 E7 oncoprotein is important for functional inactivation and is separable from proteasomal degradation of E7. J Virol 2001, 75:7583–7591
29. Wong YF, Cheung TH, Tsao GS, Lo KW, Yim SF, Wang VW, Heung MM, Chan SC, Chan LK, Ho TW, Wong KW, Li C, Guo Y, Chung TK, Smith DI: Genome-wide gene expression profiling of cervical cancer in Hong Kong women by oligonucleotide microarray. Int J Cancer 2006, 118:2461–2469
30. Grant JM: Revised FIGO staging for early invasive carcinoma of the vulva and cervix. Br J Obstet Gynaecol 1996, 103:xxi–xxii
31. Goda N, Ryan HE, Khadivi B, McNulty W, Rickert RC, Johnson RS: Hypoxia-inducible factor 1α is essential for cell cycle arrest during hypoxia. Mol Cell Biol 2003, 23:359–369
32. Akakura N, Kobayashi M, Horiuchi I, Suzuki A, Wang J, Chen J, Niizeki H, Kawamura K, Hosokawa M, Asaka M: Constitutive expression of hypoxia-inducible factor-1α renders pancreatic cancer cells

resistant to apoptosis induced by hypoxia and nutrient deprivation. Cancer Res 2001, 61:6548–6554
33. Moeller BJ, Dreher MR, Rabbani ZN, Schroeder T, Cao Y, Li CY, Dewhirst MW: Pleiotropic effects of HIF-1 blockade on tumor radiosensitivity. Cancer Cell 2005, 8:99–110
34. Semenza GL: HIF-1 and tumor progression: pathophysiology and therapeutics. Trends Mol Med 2002, 8:S62–S67
35. An WG, Kanekal M, Simon MC, Maltepe E, Blagosklonny MV, Neckers LM: Stabilization of wild-type p53 by hypoxia-inducible factor 1α. Nature 1998, 392:405–408
36. Suzuki H, Tomida A, Tsuruo T: Dephosphorylated hypoxia-inducible factor 1α as a mediator of p53-dependent apoptosis during hypoxia. Oncogene 2001, 20:5779–5788
37. Münger K, Howley PM: Human papillomavirus immortalization and transformation functions. Virus Res 2002, 89:213–228
38. Williams GH, Romanowski P, Morris L, Madine M, Mills AD, Stoeber K, Marr J, Laskey RA, Coleman N: Improved cervical smear assessment using antibodies against proteins that regulate DNA replication. Proc Natl Acad Sci USA 1998, 95:14932–14937
39. Freeman A, Morris LS, Mills AD, Stoeber K, Laskey RA, Williams GH, Coleman N: Minichromosome maintenance proteins as biological markers of dysplasia and malignancy. Clin Cancer Res 1999, 5:2121–2132
40. Ishimi Y, Okayasu I, Kato C, Kwon HJ, Kimura H, Yamada K, Song SY: Enhanced expression of Mcm proteins in cancer cells derived from uterine cervix. Eur J Biochem 2003, 270:1089–1101
41. Azar KK, Tani M, Yasuda H, Sakai A, Inoue M, Sasagawa T: Increased secretion patterns of interleukin-10 and tumor necrosis factor-α in cervical squamous intraepithelial lesions. Hum Pathol 2004, 35:1376–1384
42. Basile JR, Zacny V, Munger K: The cytokines tumor necrosis factor-alpha (TNF-α) and TNF-related apoptosis-inducing ligand differentially modulate proliferation and apoptotic pathways in human keratinocytes expressing the human papillomavirus-16 E7 oncoprotein. J Biol Chem 2001, 276:22522–22528
43. Filippova M, Song H, Connolly JL, Dermody TS, Duerksen-Hughes PJ: The human papillomavirus 16 E6 protein binds to tumor necrosis factor (TNF) R1 and protects cells from TNF-induced apoptosis. J Biol Chem 2002, 277:21730–21739
44. Woodworth CD, McMullin E, Iglesias M, Plowman GD: Interleukin 1 alpha and tumor necrosis factor α stimulate autocrine amphiregulin expression and proliferation of human papillomavirus-immortalized and carcinoma-derived cervical epithelial cells. Proc Natl Acad Sci USA 1995, 92:2840–2844
45. Peck JW, Oberst M, Bouker KB, Bowden E, Burbelo PD: The RhoA-binding protein, rhophilin-2, regulates actin cytoskeleton organization. J Biol Chem 2002, 277:43924–43932
46. Getsios S, Amargo EV, Dusek RL, Ishii K, Sheu L, Godsel LM, Green KJ: Coordinated expression of desmoglein 1 and desmocollin 1 regulates intercellular adhesion. Differentiation 2004, 72:419–433
47. Liao D, Corle C, Seagroves TN, Johnson RS: Hypoxia-inducible factor-1α is a key regulator of metastasis in a transgenic model of cancer initiation and progression. Cancer Res 2007, 67:563–572